Journal of Artificial Intelligence Practice (2026)
Clausius Scientific Press, Canada

DOI: 10.23977/jaip.2026.090107
ISSN 2371-8412 Vol. 9 Num. 1

K-means Clustering Based on Self-Sampling and Multi-Risk Minimization in NIPT Screening

Liang Hu[1], Yeqi Zhang[1], Yanyan Wu[2,3,4,*], Qian Li[2,5]

[1] *Big Data College, Fuzhou University of International Studies and Trade, Fuzhou, Fujian, China*
[2] *College of Digital Technology and Engineering, Ningbo University of Finance and Economics, Ningbo, China*
[3] *Faculty of Data Science, City University of Macau, Macau, China*
[4] *Key Laboratory of Data Science and Intelligent Computing, Fuzhou University of International Studies and Trade, Fuzhou, Fujian, China*
[5] *CKC Software Laboratory, Ningbo University, Ningbo, China*
[*] *Corresponding Author*

Keywords: NIPT; BMI Grouping; K-means, Bootstrap; Risk Minimization

Abstract: This study aimed to optimize NIPT testing strategies and mitigate clinical risks associated with individual variability and detection errors. By focusing on pregnant women carrying male fetuses, it combined Bootstrap and K-means algorithms to develop the Bootstrap K-Means method, addressing grouping biases inherent in direct clustering. The study divided maternal BMI values into four optimal groups, establishing a total risk function, time-point expectations, failure rates, and sequencing quality risk weights. By solving for the optimal NIPT testing time points for each BMI group under constrained conditions, results indicated approximately 12.3 weeks for the first three groups, with the high-BMI group delayed to 13 weeks. Sensitivity analysis demonstrated the robustness of the model outcomes. An accuracy risk function incorporating cautionary factors (advanced maternal age, obesity, non-natural conception) was developed. The failure risk function model was modified and extended to analyze optimal testing timepoints for these factors. Results indicate higher accuracy risk and model sensitivity in the high-BMI group due to its greater obesity prevalence. This optimized mathematical model for NIPT testing provides quantitative evidence to support personalized, evidence-based prenatal screening strategies in clinical practice.

1. Introduction

Non-invasive prenatal testing (NIPT) is a quite popular approach for detecting fetal genomic aneuploidies. [1]Against the backdrop of prenatal screening and eugenics, the accuracy and timing of NIPT testing are critical to safeguarding maternal and fetal health. Scientifically determining the optimal testing window and accurately diagnosing fetal chromosomal abnormalities are vital for reducing clinical risks, necessitating the development of mathematical models to support decision-making. This study aims to optimize NIPT testing strategies to mitigate risks arising from individual variability and testing errors.

2. Bootstrap-Kmeans

2.1 Bootstap

Based on the BMI values of pregnant women carrying male fetuses, the study attempted to use K-means for automatic grouping. However, considering that each pregnant woman has multiple test records and that pregnancy conditions may vary significantly among individuals, directly applying K-means for grouping may be influenced by multiple tests and individual differences, potentially leading to suboptimal grouping results.[2]

To mitigate modeling biases arising from sample imbalance and sequencing failures, this study employs bootstrap sampling. For each BMI group, data from pregnant women carrying male fetuses undergoes resampling with replacement to generate multiple pseudo-datasets. These datasets undergo repeated computations and clustering. Finally, the upper bounds of each group are averaged to obtain the final grouping results.

Bootstrapping methods enable models or algorithms to better understand the biases, variances, and characteristics inherent within them. They allow resampling to incorporate different biases, which are then treated as a unified whole.

Let the original dataset be:

$$X=\{x_1,x_2,\ldots,x_n\} \tag{1}$$

Each sample x_n corresponds to the BMI value of a pregnant woman carrying a male fetus, where n is the number of samples in that BMI group.

Perform no more than n resampling with replacement on the original dataset to generate B pseudo-datasets[3,4]:

$$X^{*(b)}=\left\{x_1^{*(b)},x_2^{*(b)},\ldots,x_n^{*(b)}\right\},b=1,2,\ldots,B \tag{2}$$

The superscript * denotes that the samples are obtained by bootstrap resampling from the original dataset. To ensure no bias in sample size during the study, exhaustive sampling was employed, meaning each pseudo-dataset contained n samples.

2.2 BMI Grouping Results Based on K-Means with Autonomous Sampling

To determine the optimal number of clusters k, i.e., the optimal number of BMI groups, this study employed the elbow method. An elbow plot was constructed by calculating the intra-cluster error sum of squares at different k values to assist in the selection process.

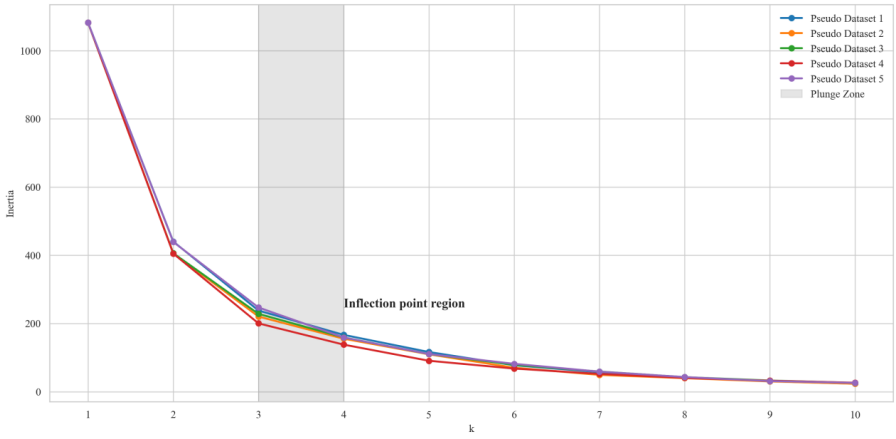

Figure 1: Elbow plots for five synthetic datasets.

Figure 1 illustrates the variation in intra-cluster error sum of squares across five synthetic datasets under different numbers of BMI clusters.

For these five datasets, the intra-cluster sum of squares decreases rapidly as the number of BMI groups increases from one. When the number of BMI groups reaches approximately four, the downward trend of the curves begins to slow significantly. This suggests that grouping the original data into four BMI categories may represent an optimal clustering approach.

K-means clustering was performed on each synthetic dataset with k set to 4. The BMI grouping results for each dataset are shown in Table 1 below:

Table 1: BMI groups and sample sizes for each dataset.

Dataset	BMI Scope	Sample Size
Dataset 1	20.70 ~30.95	427
	31.00 ~33.89	417
	33.93 ~37.64	193
	37.83 ~46.88	45
Dataset 2	20.70 ~30.12	266
	30.18 ~32.61	388
	32.65 ~35.94	305
	36.05 ~45.71	123
Dataset 3	20.70 ~30.94	400
	31.00 ~33.82	383
	33.86 ~37.49	252
	37.56 ~46.88	47
Dataset 4	20.70 ~30.66	352
	30.70 ~32.97	353
	33.01 ~35.96	263
	36.13 ~46.88	114

Calculate the upper-limit mean for each category and output the mean range; the results are shown in Table 2. Note that the lower limit of Range 1 is the minimum value of the original BMI, and the upper limit of Range 4 is the maximum value of the original BMI.

Table 2: BMI Grouping Results.

BMI Interval	Scope
Interval 1	20.70~30.73
Interval 2	30.73~33.40
Interval 3	33.40~36.93
Interval 4	36.93~46.88

Based on the above analysis, this study ultimately divided the BMI data of pregnant women carrying male fetuses into four groups: 20.70–30.73, 30.73–33.40, 33.40–36.93, and 36.93–46.88.

3. Optimal Timing for NIPT Testing

3.1 Definition of Decision Variables

To develop an optimal timing strategy for testing, screening timepoints must be determined for pregnant women in different BMI groups at various gestational weeks. Therefore, the decision variable can be set as the i-th BMI group undergoing NIPT testing at the t-th gestational week, denoted as t_i.

3.2 Point-in-Time Expected Risk

In clinical practice, the early detection of fetal abnormalities is crucial for timely intervention and treatment. Based on medical experience:

Early screening (≤12 weeks): Lower risk, ample intervention window.

Mid-term screening (13–27 weeks): Gradually increasing risk, greater difficulty in intervention.

Late screening (≥28 weeks): Extremely high risk, potential loss of therapeutic window.

Gestational age itself is a critical factor influencing test efficacy and clinical risk. To quantify this impact in the model, we constructed a time-dependent expected risk function for gestational age t_i to penalize late screening and incentivize earlier testing. Based on risk levels across screening periods, the following risk expectation formula was designed:

$$E(t) = w_1 \cdot P(t \le 12) + w_2 \cdot P(13 \le t \le 27) + w_3 \cdot P(t \ge 28) \tag{3}$$

Among these, w_1, w_2, and w_3 represent the risk weights for different time periods, satisfying $w_1 < w_2 < w_3$, reflecting the increasing risk relationship between early, mid, and late screening. P(t) denotes the risk probability when screening is conducted at gestational week t.

$$E(t) = \begin{cases} 0.3, & t<12 \\ 0.6+0.05(t-12), & 12 \le t \le 27 \\ 1.0+0.1(t-28), & t>27 \end{cases} \tag{4}$$

Based on medical experience and literature data, this paper sets specific risk weight values as $w_1 = 0.3$, $w_2 = 0.6$, and $w_3 = 1.0$. Assuming risk probability changes linearly across time periods, a piecewise function form for the point-in-time expected risk function is derived.

To simplify the model, the point-in-time expected risk function is further streamlined into a continuous exponential function. This function exhibits a growth pattern characterized by initial slow growth followed by accelerated growth, effectively simulating the rapid increase in risk during later periods. The specific form is as follows:

$$E(t) = A + B \cdot e^{k(t-t_0)} = 0.3 + e^{0.1(t-12)} \tag{5}$$

Here, A represents the baseline risk level, B denotes the growth margin used to control the starting point of risk increase, k signifies the growth rate used to adjust the pace of risk escalation, and t_0 serves as the reference time point for gestational weeks.

3.3 Risk of Failure

In NIPT testing for male fetuses, fetal Y chromosome concentration reaching the threshold (≥4%) is the core indicator for determining test reliability. If the concentration fails to meet the threshold, sequencing results may be inaccurate or fail, impacting clinical decision-making.

Therefore, a linearly inverted failure risk function must be incorporated into the model to quantify the probability of test failure due to insufficient Y concentration at gestational week t. The formula is as follows:

$$F(t) = 1 - P_i(t) \tag{6}$$

Here, $P_i(t)$denotes the probability that the Y chromosome concentration meets the standard at gestational week t for the i-th sample or BMI group. A higher probability indicates lower failure risk, while a lower probability signifies higher failure risk.

$P_i(t)$ requires estimation using historical data. Given the limited effective data in this study, machine learning methods were not considered for probability prediction. Instead, the Naive Bayes statistical method was employed for estimation.

3.4 Naive Bayes Probability Calculation

The probability of meeting the standard $P_i(t)$can be estimated using the Naive Bayes method. Assuming gestational age t and BMI value are the primary factors influencing the concentration of Y meeting the standard, and that they are mutually independent, we have:

$$P_i(t) = \frac{n_{\text{pass}}+\alpha}{n_{\text{total}}+\alpha+\beta} \tag{7}$$

Here, n_{pass} denotes the number of samples meeting the Y concentration threshold at gestational week t and BMI group i, while n_{total} represents the total sample size for that group. α and β are Bayesian smoothing parameters used to avoid the zero probability issue.

3.5 Sequencing Quality Risks

The quality of sequencing data directly impacts the accuracy of chromosome concentration assessment, with GC content deviation being the primary factor leading to sequencing failure or misjudgment. This paper constructs a sequencing quality risk function for gestational week t to penalize substandard sequencing quality:

$$\text{G}(t) = \sigma(GC(t)\text{-}0.5)^2 \tag{8}$$

$GC(t)$ denotes the GC content at gestational week t, where 0.5 represents the ideal central value for GC content. σ is a penalty coefficient that amplifies the risk of deviation; a larger σ indicates greater sensitivity to deviations.

To ensure the function is continuous and differentiable across its entire domain while maintaining good smoothing properties, a squared operation is introduced in the penalty term to facilitate more efficient convergence. This makes the function more sensitive to GC content deviations from the center value, enabling it to distinguish between minor and severe deviations.

3.6 Constraints

During model solution, the following constraints must be satisfied:

(1) Gestational age range constraint: For each BMI group, the detection time point t_i must fall within the clinically permissible detection time range, i.e.,

$$t_i \in [10,28] \tag{9}$$

Where t_i denotes the gestational week at the optimal detection time point for the i-th BMI group.

(2) Compliance rate constraint: The compliance rate of Y chromosome concentration at the optimal detection time point for each group must not fall below the minimum clinical requirement (≥ 0.4) to ensure the reliability of detection results.

(3) Sequencing Quality Constraints: The GC content at the detection time point must fall within a reasonable range, satisfying:

$$0.4 \leq \text{GC}(t_i) \leq 0.6 \tag{10}$$

Where $\text{GC}(t_i)$ denotes the GC content at gestational week t_i.

By performing a weighted sum of the above three risk functions, the total risk function is obtained:

$$minR_i(t)=\alpha \cdot E(t)+\beta \cdot F(t)+\gamma \cdot G(t) \tag{11}$$

$$\text{s.t.}\begin{cases} t_i^*=\arg\, minR_i(t) \\ t_i \in [10,28] \\ P_i(t_i)\geq 0.4 \\ 0.4\leq GC(t_i)\leq 0.6 \end{cases} \tag{12}$$

Among these, α, β, and γ represent the weighting coefficients for point-in-time expected risk, failure risk, and sequencing quality risk, respectively, reflecting the relative importance of each risk factor within the overall risk. t_i^* denotes the optimal testing time point for the i-th BMI group. By solving this optimization problem, the optimal NIPT testing time for each BMI group can be determined, thereby reducing clinical risk while enhancing the success rate and accuracy of the test.

3.7 Optimal NIPT Testing Timing for Each BMI Group

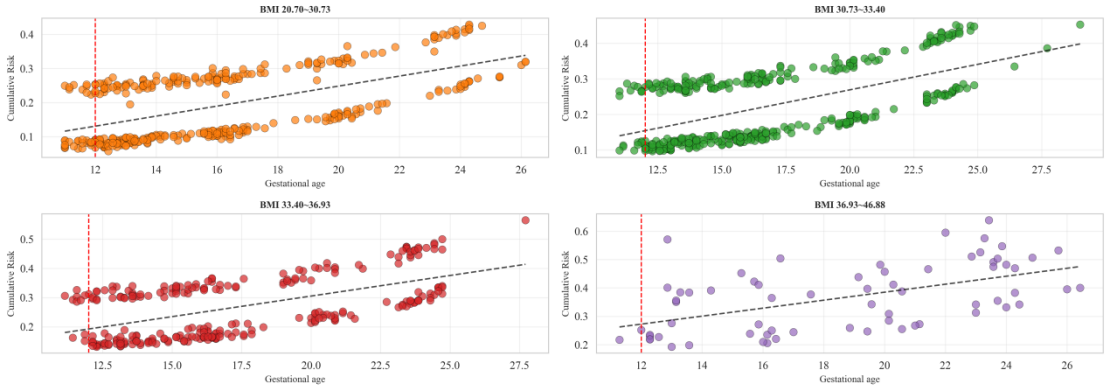

Figure 2: Relationship between Gestational Age and Overall Risk.

Analysis of Figure 2 reveals that the optimal testing window for the first three BMI groups occurs around 12.3 weeks, while the recommended timing for the highest BMI group is delayed to 13 weeks. This delay likely stems from lower fetal DNA concentrations in the blood of high-BMI pregnant women, requiring a longer gestational period to accumulate sufficient levels for accurate detection. Testing earlier than this threshold may result in failure or inaccuracy due to insufficient concentration.

This paper employs Monte Carlo methods to conduct sensitivity analysis on the error parameters within the model. The error parameters are as follows:[5]

(1) Sequencing error (σ): Reflects potential systematic errors during sequencing, affecting the accuracy of GC content estimation. It follows a normal distribution N(1.0, 0.2).

(2) Risk weights (α, β, γ): Corresponding to the weighting coefficients for expected risk, failure risk, and sequencing quality risk at each time point, reflecting the relative importance of each risk in the total risk. The parameters are uniformly distributed within the intervals [0.3, 0.5], [0.3, 0.5], and [0.1, 0.3], respectively.[6,7]

Perform 1000 random samples within the error range for each parameter. The study calculated the optimal NIPT testing time point for each BMI group under each sample, yielding the optimal time point range and standard deviation for each group as shown in Table 3.

Table 3: Optimal time window for each BMI group.

BMI Grouping	Optimal timing window	Optimal timing on average	Standard deviation
20.70~30.73	12.43~12.43	12.43	0.09
30.73~33.40	11.00~12.57	12.02	0.63
33.40~36.93	12.29~13.14	12.41	0.30
36.93~46.88	13.00~16.14	13.02	0.22

The standard deviation for the optimal timing in the 20.70–30.73 group is only 0.9, indicating highly stable results within this group. Standard deviations for all other groups are less than 1, demonstrating that the model is insensitive to error parameters and yields robust results.

4. NIPT Risk Minimization Extension

4.1 Accuracy Risk Function

According to the Technical Specifications for Prenatal Screening and Diagnosis Using Fetal Free DNA in Maternal Peripheral Blood established by China's National Health and Family Planning Commission in 2016[8], the following categories of pregnant women are considered groups for whom NIPT should be used with caution:

(1) Pregnant women aged 35 or older at the estimated date of delivery;

(2) Pregnant women with severe obesity (BMI > 40);

(3) Pregnant women conceived through non-natural reproductive methods.[9]

Individuals with the above conditions are considered a cautionary group, and the accuracy of testing may be somewhat reduced when conducting tests. [10,11]

This paper introduces an accuracy risk function to the original objective function, imposing additional penalties on populations requiring cautious treatment. The specific formula is as follows:

(1) Age offset: Penalties apply only to pregnant women aged ≥35.

$$f_{Age} = \left(max\left(0, \frac{\text{Age}_i\text{-}35}{\sigma_{\text{Age}}}\right)\right)^2 \tag{13}$$

Here, Age_i denotes the age of the i-th pregnant woman, and σ_{Age} represents the standard deviation of age.

(2) BMI penalty: Applies only to pregnant women with a BMI > 40.

$$f_{BMI} = \left(max\left(0, \frac{W_i}{H_i^2}\text{-}\mu_{BMI}\right)\right)^2 \tag{14}$$

Among these, μ_{BMI}=40 represents the BMI threshold for obesity, where W denotes weight and H denotes height.

(3)IVF Penalty: Binary variable, where natural conception is 0 and IVF or IUI is 1.

$$f_{ivf} = \begin{cases} 1, & \text{IVF, IUI} \\ 0, & Natural\ conception \end{cases} \tag{15}$$

Multiply all three components uniformly by the weighting coefficient λ to obtain the final accuracy risk function:

$$T_i(t) = \lambda \left[\left(max\left(0, \frac{\text{Age}_i\text{-}35}{\sigma_{\text{Age}}}\right)\right)^2 + \left(max\left(0, \frac{W_i}{H_i^2}\text{-}\mu_{BMI}\right)\right)^2 + \text{IVF}_i \right] \tag{16}$$

4.2 Modification of the Failure Risk Function

When no prior information is available (α=β=0), Bayes' theorem degenerates into a frequentist estimation form. The calculated result is equivalent to the compliance rate, where the compliance rate $T_i(t)$ is regarded as the posterior probability estimate for the Y concentration meeting the standard.[12]

The original function can be reformulated as a joint penalty term for individual achievement probability and group achievement proportion, yielding:

$$F(t)=\left(1-P_i(t)\right)\left(1-\frac{n_{\text{pass}}(t)}{n_{\text{total}}(t)}\right) \tag{17}$$

Based on the above analysis, the new total risk function after modification is as follows:

$$minR_i(t)=\alpha\cdot E(t)+\beta\cdot F(t)+\gamma\cdot G(t)+\lambda\cdot T(t) \tag{18}$$

$$\text{s.t.}\begin{cases} t_i^*=\arg\, minR_i(t) \\ t_i\in[10,28] \\ P_i(t_i)\geq 0.4 \\ 0.4\leq GC(t_i)\leq 0.6 \\ \dfrac{n_{\text{pass}}}{n_{\text{total}}}\geq P_{\min} \end{cases} \tag{19}$$

4.3 Optimal NIPT Testing Timing under Precautionary Considerations

Calculate the total risk function $R_i(t)$ for the newly added accuracy risk T(t). The accuracy risk values within each BMI group and the proportion of cautionary factors are shown in Table 4:

Table 4: Average accuracy risk and proportion of high-risk factors across BMI groups.

BMI Grouping	Average Accuracy Risk	Proportion of factors requiring careful consideration		
	Risk Value	Advanced Age	Obesity	IVF
20.70-30.73	0.0011	4.13%	0.00%	2.48%
30.73-33.40	0.0024	6.67%	0.00%	1.79%
33.40-36.93	0.0012	8.02%	0.00%	0.38%
36.93-46.88	0.0702	4.48%	26.87%	0.00%

The first three groups exhibited low average accuracy risk with 0% obesity prevalence. In the fourth group, accuracy risk surged to 0.0702, accompanied by a 26.87% obesity rate. Meanwhile, advanced maternal age and IVF rates showed no discernible pattern and remained generally low, indicating they were not primary risk factors.

Table 5: Optimal NIPT Testing Range under Precautionary Considerations.

BMI Grouping	Optimal timing window	Optimal timing on average	Standard deviation
20.70-30.73	11.00~13.00	12.26	0.42
30.73-33.40	11.00~12.57	11.30	0.37
33.40-36.93	11.14~13.43	12.11	0.36
36.93-46.88	11.29~16.29	13.07	0.82

Compared with the sensitivity analysis results in Table 3, the optimal timing error range for the first three groups has widened, as shown in Table 5.

The standard deviation for the 36.93–46.88 group was 0.22 in Table 3, but increased significantly to 0.82 in the subsequent table. The average optimal detection time point for the 30.73–33.40 group was 11.3 weeks, advancing by 0.72 weeks compared to the baseline model's 12.02 weeks. This outcome resulted from the combined effects of "clinically permissible physiological conditions" and "optimal model risk balance," remaining within the range of normal clinical variability.

5. Model Evaluation and Deployment

5.1 Advantages of the Model

(1) The objective function integrates expected risk, failure risk, sequencing quality risk, and accuracy risk, with each risk component adjustable via weighting coefficients for enhanced interpretability.

(2) Most risk factors are expressed as continuous functions, avoiding discrete jumps. This enhances universality and facilitates computation.

(3) The model structure supports adding new risk factors, ensuring good scalability.

(4) Each sub-item can be independently analyzed, debugged, and subjected to sensitivity assessment, enabling model iteration and optimization.

(5) Through autonomous sampling, the impact of repeated testing and individual variations on detection results is minimized as much as possible.

5.2 Model Limitations

(1) The current failure risk function models the product of individual probability and population proportion, potentially leading to information redundancy or numerical instability.

(2) Statistical fluctuations in population proportion may compromise the robustness of optimization results.

(3) Some weights are not data-fitted, and their assignment may introduce subjective bias; careful selection and validation are required.

5.3 Application Promotion

(1) Use logistic regression, random forest, or Bayesian models to fit the weights of each risk factor, enhancing the model's objectivity.

(2) Encapsulate each risk factor as an independent module to support flexible combination and replacement.

(3) Enable or disable accuracy risk factors or population proportion constraints based on different clinical requirements.

6. Conclusion

The Bootstrap K-Means clustering method effectively addresses clustering issues caused by sample imbalance and individual detection variations. Through resampling with replacement and multiple iterations using male fetus BMI data, four optimal BMI groups were identified: 20.70–30.73, 30.73–33.40, 33.40–36.93, 36.93–46.88.

By constructing a total risk function incorporating timing expectations, failure rates, and sequencing quality, and integrating constraints such as clinical gestational age, pass rate, and sequencing quality, the optimal NIPT testing timing for each BMI group can be determined. The optimal testing timing for the lowest and middle BMI groups occurs at 12.3 weeks. For the high BMI group, where fetal Y chromosome accumulation progresses more slowly, delaying the optimal timing to 13 weeks. Monte Carlo sensitivity analysis indicates the model exhibits low sensitivity and robust performance.

The accuracy risk function incorporating cautionary factors (advanced maternal age, severe obesity, non-natural conception) and the failure risk modification function integrating individual and population pass rates enhance the quantification of NIPT testing risks. The expanded model reflects

the impact of cautionary factors. The 26.87% prevalence of severe obesity in the high-BMI group constitutes the primary source of accuracy risk. This model exhibits slightly reduced sensitivity to error parameters, while accuracy risks remain low across other subgroups.

Acknowledgments

This research was supported by the Scientific Research Project of Zhejiang Provincial Department of Education [GrantNo. Y202559174], [Grant No. Y202559152]; Open Research Project of Key Laboratory of Data Science and Intelligent Computing, Fuzhou University of International Studies and Trade [Grant No.SZ2025001].

References

[1] Xue Z ,Zhou A, Zhu X, et al. NIPT-PG: empowering non-invasive prenatal testing to learn from population genomics through an incremental pan-genomic approach [J]. Briefings in bioinformatics,2024,25(4).
[2] Fukuchi I J. Approximate Selection of All Populations Better Than a Control by Bootstrap[J]. Sankhya A, 2025,87(2):1-20.
[3] Wywiał J, Szkutnik T. Bootstrap tests for unbiasedness of predictors[J]. Communications in Statistics - Simulation and Computation,2025,54(6):1987-2004.
[4] FeinbergM, Cl ́menençonS, RudazS, et al. Kernel-Based Bootstrap Synthetic Data to Estimate Measurement Uncertainty in Analytical Sciences[J]. Journal of Chemometrics,2024,38(12):e3628.
[5] Wei Z, Tima M, Julie S, et al.Cost-effectiveness of prenatal screening and diagnostic strategies for Down syndrome: A microsimulation modeling analysis [J]. PloS one,2019,14(12):e0225281.
[6] Cogno N, Bauer R, Durante M . Mechanistic model of radiotherapy-induced lung fibrosis using coupled 3D agent-based and Monte Carlo simulations [J].Communications medicine,2024,4(1):16.
[7] Kwan Y L, Joo O K, Mi-Kyung L, et al. Estimating the measurement uncertainties of the international sensitivity index of 12 thromboplastins through Monte Carlo simulation [J]. Thrombosis Research,2023,224:32-37.
[8] Chen Jue, Zhu Liping, Cen Shuyuan, et al. Noninvasive prenatal screening using fetal cell-free DNA in maternal peripheral blood: A study of 21,092 cases [J]. Chinese Journal of Prenatal Diagnosis (Electronic Edition), 2023, 15(01): 29-34.
[9] You Zuping, Wang Zheng. Analysis of the Establishment of Institutions and Current Status of Prenatal Screening Using Fetal Cell-Free DNA in Peripheral Blood of Pregnant Women in Jinhua City [J]. Chinese Journal of Health Supervision, 2021, 28(02): 116-121.
[10] Zhai Chunya. Clinical Application Research of Non-Invasive Prenatal Testing (NIPT) in Sex Chromosome Abnormalities [D]. Tianjin Medical University,2021.
[11] Pang Yu. Clinical Application of Non-Invasive Prenatal Testing in Fetal Chromosomal Disease Screening [D]. Anhui Medical University, 2022.
[12] Tarasi L, Covelli M, Fatis D T C, et al. Prior Information Shapes Perceptual Confidence.[J].Journal of cognition,2025,8(1):11.